Experimental study of two-fluid effects on magnetic reconnection in a laboratory plasma with variable collisionality

Masaaki Yamada, Yang Ren, Hantao Ji, Joshua Breslau, Stefan Gerhardt, Russell Kulsrud, and Aleksey Kuritsyn
Center for Magnetic Self-Organization in Laboratory and Astrophysical Plasmas, Princeton Plasma Physics Laboratory, Princeton University, Princeton, New Jersey 08543

(Received 14 March 2006; accepted 24 March 2006; published online 26 May 2006)

This article describes the recent findings on two-fluid effects on magnetic reconnection in plasmas with variable collisionality in the magnetic reconnection experiment (MRX) [M. Yamada *et al.*, Phys. Plasmas **4**, 1936 (1997)]. The MRX device has been upgraded to accommodate a variety of reconnection operation modes and high energy density experiments by increasing its capacitor bank energy and extending the discharge duration. As our experimental operation regime has moved from the collisional to the collision-free, two-fluid effects have become more evident. It is observed that the two-dimensional profile of the neutral sheet is changed significantly from the rectangular shape of the familiar Sweet-Parker type to a double wedge shape as the collisionality is reduced and the reconnection rate increases. The recent evolution of our experimental research from the magnetohydrodynamics (MHD) to the two-fluid analysis is presented to illuminate the physics of Hall MHD in a collision-free reconnection layer. In particular, a clear experimental verification of an out-of-plane quadrupole field, a characteristic signature of the Hall MHD, has been made in the MRX neutral sheet, where the sheet width is comparable to the ion skin depth. It is important to note that the Hall effect, which occurs due to two-dimensional laminar flows of electrons in the reconnection plane, is observed together with the presence of low and high frequency magnetic turbulence, which often has three-dimensional structures. These observations in MRX have striking similarities to the recent magnetospheric measurements of reconnection region, in which the quadrupole component has been detected together with magnetic fluctuations. © *2006 American Institute of Physics*. [DOI: 10.1063/1.2203950]

I. INTRODUCTION

In hot conductive plasmas described by ideal magnetohydrodynamics (MHD), magnetic field lines are strongly frozen into and move together with the plasma. The contrary process to this occurs during magnetic reconnection, which allows these lines to break, change their topology, and self-organize, releasing large amounts of magnetic energy. The magnetic reconnection phenomenon has wide-ranging importance[1–4] in the universe and is considered to be a key process in the evolution of solar flares,[5–9] in the dynamics of the earth's magnetosphere,[10,11] and in the formation process of stars.[4] It also occurs as one of the most important self-organization processes in fusion research plasmas and often plays a key role in ion heating, as well as in determining confinement properties of hot plasmas.[3]

A current sheet, or neutral sheet, often manifests the essential physics of magnetic reconnection.[1–4] In this magnetic reconnection region, the interplay between magnetic fields and plasma particles takes place and the key physics of their interaction can be studied. Figures 1(a) and 1(b) present two typical current sheet model patterns in which magnetic fields of opposite polarity approach a region where they merge and reconnect. The newly reconnected field lines emerge from the reconnection region and move away.

In the MHD formulation, the motion of magnetic field lines in a plasma can be described by combining Maxwell's equations and Ohm's law,

$$\mathbf{E}+\mathbf{v}\times\mathbf{B}=\eta\mathbf{j}, \tag{1}$$

$$\partial\mathbf{B}/\partial t=\nabla\times(\mathbf{v}\times\mathbf{B})+(\eta/\mu_0)\nabla^2\mathbf{B}. \tag{2}$$

When $\eta=0$, Eq. (2) states that magnetic field lines move with the fluid as elaborately discussed by Parker.[1] In resistive MHD plasmas, hydromagnetic flows can lead to the formation of a neutral sheet such as shown in Fig. 1(a) where the transverse plasma flow is reduced to near zero and the electric field ($\mathbf{E}$) is balanced with $\eta\mathbf{j}$ in Eq. (1). In this diffusion region, the effect of resistivity becomes sufficiently large that a magnetic field line can lose its original identity and reconnect to another field line. Sweet and Parker developed a two-dimensional (2D) incompressible MHD model.[12,13] They assumed that the local reconnection rate can be described by a steady state ($\partial\mathbf{B}/\partial t=\partial\mathbf{v}/\partial t=0$) formulation through collisional dissipation. Utilizing the continuity equation and pressure balance between the upstream ($P\sim B^2/2\mu_0$) and the downstream dynamic pressure ($P\sim\rho V^2/2$), they derived a very simple formula for the reconnection speed[1,12,13]:

$$V_{\mathrm{reco}}/V_{\mathrm{A}}=(\eta/\mu_0 L V_{\mathrm{A}})^{1/2}=S^{-1/2}, \tag{3}$$

where $S\equiv\tau_D/\tau_{\mathrm{A}}\gg 1$ for MHD plasmas (L is the plasma sheet length; $\tau_D\equiv\mu_0 L^2/\eta$ is the diffusion time; and $\tau_{\mathrm{A}}\equiv L/V_{\mathrm{A}}$ is the Alfvén transit time). According to their resistive MHD formulation, magnetic fields dissipate in the rectangular reconnection region [Fig. 1(a), red dashed line] where incoming plasma flux is balanced with the outgoing

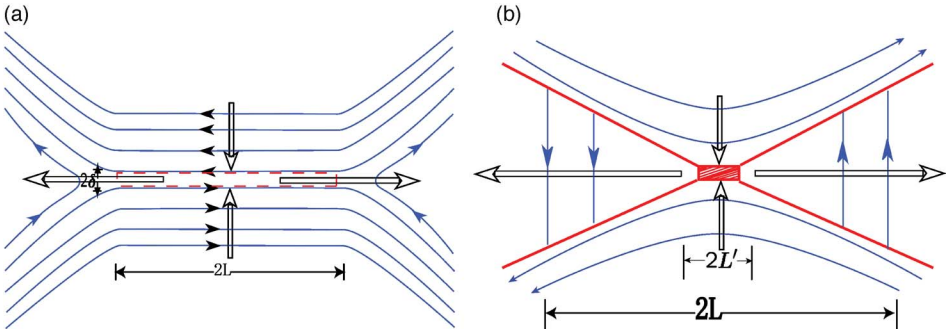

FIG. 1. (a) Sweet-Parker and (b) Petschek models.

flux satisfying a continuity equation for plasma fluid.

In the Sweet-Parker model, the reconnection rate depends on the Lundquist number S, the ratio of the resistive diffusion time (based on particle collisions) to the crossing time of Alfvén waves. In astrophysical plasmas, S is usually extremely large: S can be 10^8-10^{14} in solar flares, and $10^{15}-10^{20}$ in the galaxy. Magnetic reconnection in the Sweet-Parker model occurs far too slowly $[\tau_{\mathrm{rec}} \sim S^{1/2}\tau_{\mathrm{A}}]$ to explain reconnection phenomena in solar flares, star formation, or astrophysical dynamos. For instance, in actual solar flares, reconnection occurs much faster (<1 h) than the Sweet-Parker time (0.1-1 year). The slowness of the Sweet-Parker reconnection model comes from the assumption that plasma and magnetic flux have to go through the narrow neutral sheet shown in Fig. 1(a) with thickness of $\delta = L/S^{1/2}$. For this reason another theory was proposed by Petschek[14] only a few years later, introducing shocks which open up the neutral sheet to a wedge shape as is shown in Fig. 1(b). This opening of the outflow region leads to a much faster rate of reconnection. This theory, whose time scale is consistent with the observed fast reconnection rate in space, has been very popular, but it has not yet been rigorously established because it is not compatible with resistive MHD characteristics.[4] However, with a locally enhanced resistivity in the neutral region, some MHD theories lead to the Petschek type shock region.[15] To date, the shock structure, an outcome of the Petschek type model, has not been identified in laboratory experiments.

For a long time magnetic reconnection has been generally described through the standard MHD theory that treats the plasma as a single fluid. The MHD framework is based on the assumption that electrons and ions move together as one fluid even in the presence of internal current, and is generally regarded as a good approximation to describe the global plasma dynamics. But this condition does not hold in a thin collision-free reconnection layer since ions can become demagnetized, moving quite differently from electrons, and the relative drift velocity between electrons and ions can be very large ($\sim V_A$). Reconnection layers such as those created at the magnetopause[10] by the interaction of incoming solar winds with the earth dipole field, become very thin, comparable to the ion skin depth (c/ω_{pi}). In this high beta region, the ion skin depth is comparable to the ion gyroradius and only electrons are magnetized. This separation of ion and electron motions leads to the Hall effect. This effect becomes so dominant that it can be considered as one of the important mechanisms for speeding up the rate of reconnection.[16] Beginning with earlier work by Sonnerup[17] and Terasawa,[18] extensive theoretical and numerical work has been carried out over the past two decades on the two-fluid effects in the small critical layer where reconnection occurs. Also, electromagnetic and/or electrostatic turbulence at high frequency ($\omega > \omega_{ci}$) can be excited and increase the magnetic reconnection rate. In the recent literature the above two mechanisms have been often cited as possible causes for fast reconnection: anomalous resistivity generated by plasma turbulence and the Hall effect of two-fluid theory.[16] We note that there can be overlaps between these mechanisms when the plasma turbulence is described by a two-fluid formulation. In such cases, both mechanisms can be considered as two-fluid effects in a broad sense. In the past decade, several dedicated experimental studies have been carried out to investigate the key physics of the current sheet in the two fluid regime.[19]

Sonnerup[17] first pointed out that the Hall effect can produce an out-of-plane quadrupole magnetic field in the diffusion region and he argued that the ion and electron skin depth scales may control the structure of the diffusion region, but he did not elaborate on the role of the Hall effect in magnetic reconnection. Later on, Terasawa[18] using a 2D eigenmode analysis studied the Hall effect in the tearing mode instability and concluded that the Hall effect not only produces the quadrupole magnetic field, but also increases the reconnection rate. However, the mechanism how the Hall effect facilitates reconnection was not clear. A decade later Drake *et al.*[20] observed the generation of the quadrupole magnetic field in a numerical simulation but the role of the Hall effect in determining the reconnection rate had not been fully understood. Mandt *et al.*[21] showed a simple physical mechanism how the Hall effect can bend field lines and drive reconnection based on numerical results. Biskamp *et al.*[22] using a two-fluid analysis found that the reconnection rate is Alfvénic and is determined by the larger-scale ion dynamics. Then under the GEM (Geospace Environment Modeling) reconnection challenge program, Birn *et al.*[16] concluded that the Hall effect is the basic mechanism which drives fast magnetic reconnection, that the reconnection rate is controlled by ion dynamics, and that it is not sensitive to the dissipation mechanism happening at the electron skin depth scale. One caution we must remember is that all the simulations mentioned above used 2D geometry. The important physics associated with the third dimension such as current-driven instabilities was ruled out. Although there is ample evidence

for the Hall effect from both space observations[23–25] and experiments,[26–28] the picture of fast magnetic reconnection is far from complete.

In the magnetopause, the two-fluid physics were analyzed in terms of the ion diffusion region of scale size c/ω_{pi}, ~100 km and the electron diffusion region of scale size c/ω_{pe}, ~2 km. The ion diffusion region was observed at the subsolar magnetopause to have the properties expected from Hall MHD theory.[25] When the polar satellite crossed through magnetopause region, an out-of-reconnection plane Hall magnetic field was recorded near the separatrices of the current sheet. However this observation is very rare, since it is difficult to determine the exact path of the measuring satellites when they cross the neural sheet. Even with the cluster satellites, measurements often suffer from not knowing where in the reconnection geometry the measurements were made. In laboratory experiments, the locations of probes and/or detectors are easily determined relative to the reconnection layer.

One of the main objectives of the present article is to evaluate the effects of Hall physics on magnetic reconnection without a guide field in the magnetic reconnection experiment (MRX).[29] Another goal is to identify criteria for the transition from the regimes where reconnection is described by one-fluid resistive MHD to those described by two-fluid theory. One important parameter is the relative size of the ion skin depth with respect to the Sweet-Parker layer width. This ratio is found to be proportional to the square root of the ratio of the electron mean free path to the neutral sheet length (~system size). In this work an experimental study is carried out to find out how magnetic reconnection depends on this parameter. In Sec. II two-fluid physics and analysis is extensively discussed. Our experimental setup is presented in Sec. III and experimental results in Secs. IV and V, followed by summary and discussions in Sec. VI.

II. TWO-FLUID FORMULATION

It is recognized that a detailed analysis of a thin reconnection layer should illuminate the physics of the two-fluid dynamics for reconnection. It has been observed in the MRX[29–31] as well as in the earth magnetosphere[23–25] that the width of the reconnection region such as shown in Fig. 1 is on the order of the ion skin depth as well as the ion gyroradius. In the relatively collisional regime, the profiles of reconnection field have been found to be consistent with the Harris sheet[31] based on kinetic theory for electrons and ions.

The two-fluid dynamics can be described by the "generalized" Ohm's law. The generalized Ohm's law, which describes force balance on an electron fluid, is given by

$$\mathbf{E}+\mathbf{V}\times\mathbf{B}=\eta_s\mathbf{j}+(\mathbf{j}\times\mathbf{B})/en+m_e/e(\partial\mathbf{v_e}/\partial t+\mathbf{v_e}\cdot\nabla\mathbf{v_e})-\nabla\cdot\mathbf{P_e}/en. \quad (4)$$

Here, the conventional notations are used for local electric field and magnetic field vectors, **E**, **B**; current density, **j**; plasma flow velocity, **V**; electron flow velocity, $\mathbf{v}_e$; and electron pressure tensor, $\mathbf{P_e}$. Generally in Eq. (4), all quantities include fluctuation components. The resistivity η_s denotes the classical Spitzer resistivity based on Coulomb collisions.

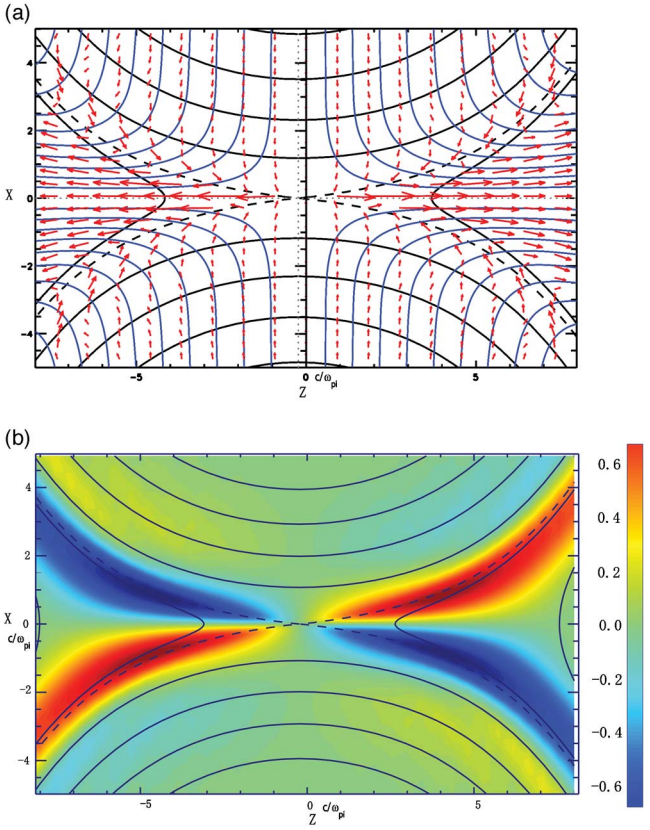

FIG. 2. (a) The results from a two fluid simulation (Ref. 38). Patterns of ion (blue lines) and electron (red arrows) fluid flows in the neutral sheet superposed on the flux plot of reconnection field lines (black). The dashed lines indicate the separatrix. The coordinates are in unit of $\delta_i=c/\omega_{pi}=1.0$. (b) The out-of-plane quadrupole (B_y) is shown in color coded contours together with in-plane magnetic field lines. The 3D magnetic field lines are pulled by electrons flowing in the y (out-of-sheet) direction of the neutral sheet.

In a thin reconnection layer in which the ions and electrons do not move together, new effects associated with the Hall term in the generalized Ohm's equation (the second term on the right-hand side) contributes to a large electric field in the direction of sheet current. This large electric field represents the fast motion of flux lines, or a fast rate of magnetic reconnection; $E=-d\Psi/dt$, where Ψ is the magnetic flux function.

Recent 2D numerical simulations[16,32–37] of the collision free neutral sheet based on two-fluid or kinetic codes demonstrate the importance of the Hall term ($\mathbf{j}\times\mathbf{B}$) through a steady (laminar) cross-field current of electrons, which contributes to a large apparent resistivity and generates fast reconnection. A recent 2D numerical study demonstrates the essence of the two-fluid dynamics in the reconnection region, although the dissipation mechanisms at the center of reconnection region are as yet to be determined.[38]

The two-fluid dynamics of reconnection are understood as illustrated in Fig. 2(a). As the reconnecting field lines move into the neutral sheet of width comparable to the ion skin depth and approach the X point (center of the reconnection plane), ions become demagnetized. These ions gradually change their flow direction by 90°, from the x to the z direction in the reconnection (x,z) plane. It is shown that magnetized electrons flow quite differently still following magnetic field lines until they approach the X point [strictly speaking,

"*X* line" in three-dimensional (3D) geometry] or separatrix lines (likewise separatrix surfaces in 3D). Although the ion gyroradius is comparable to the thickness of the reconnection layer, so that unmagnetized ions present a smooth density throughout the layer, electrons are strongly controlled by the magnetic field. As the electrons' $E_y \times B_z$ motion makes them to migrate toward the *X* line, the magnetic field weakens and the electron's drift (E_y/B_z) becomes larger, accelerating electrons near the *X* line (which extends in the *y* direction). With magnetic reconnection, the accelerated electrons are ejected along the *z* axis. This electron flow patterns shown in Fig. 2(a) generates an out-of-plane magnetic field with a quadrupole profile, and this effect has been regarded as a signature of the Hall effect.[16,32–36] This process can be interpreted as a mechanism in which the electrons, which are flowing in the direction of the neutral sheet current, tend to pull magnetic field lines toward the direction of electron sheet current, the *y* direction.[21]

As is shown in Fig. 2(a), the electrons which flow through these separatrix regions tend to be accelerated at first toward the *X* line. Then after making sharp turns at the separatrix, they flow outward in the *z* direction. Here we note that this effect is strong when the electron current is caused by $E_x \times B_z$ drift, but this explanation is not valid when the electron current is caused only by the diamagnetic current flow. Although this effect has been observed sometimes in the magnetosphere plasma,[25,39] it has not been observed in laboratory plasmas until recently.[26–28] In Fig. 2(b) the color coded contours present a 2D profile of the out-of-plane quadrupole generated by the differential electron and ion flows. The amplitude of the out-of-plane field becomes the largest around the separatrix regions as indicated in Fig. 2(a). If one displayed a 3D magnetic field line configuration, it would demonstrate clearly that the electrons pull magnetic field lines toward the direction of electron sheet current. Recently Uzdensky and Kulsrud[49] developed an analytical theory to describe the characteristics of the out-of-plane quadrupole field generated by the flow of electrons in the reconnection plane in which unmagnetized ions present a smooth density throughout a layer.

In addition to the laminar Hall effect discussed previously, we expect that the fluctuation components of $\mathbf{j}_e \times \mathbf{B}$, $en(\mathbf{v}_e \cdot \nabla \mathbf{v}_e)$, and $\nabla \cdot \mathbf{P}_e$, $en\mathbf{E}$ can make a notable contribution to the electrons' force balance and the energy dissipation rate, thus influencing the magnetic reconnection speed. Equation (4) can be expressed in a similar form to that of the resistive MHD, if we express the right-hand side as $\eta_s \mathbf{j} + \eta_{\mathrm{anom}} \mathbf{j} = \eta_{\mathrm{eff}} \mathbf{j}$, where the crucial fluctuation terms in $\mathbf{j}_e \times \mathbf{B} + m_e/e$ and $(\partial \mathbf{v_e}/\partial t + \mathbf{v}_e \cdot \nabla \mathbf{v_e}) - \nabla \mathbf{P_e}/en - e\mathbf{E}/e n_o$, are (nonlinearly) proportional to the driving term, the electron current density $j_y (\sim v_{ey})$, and can be expressed together as $\eta_{\mathrm{anom}} j_y$. We note that the fluctuation-induced resistivity should include $\langle n_1 E_{1y} \rangle / n_0$, where n_1 and E_1 are fluctuating density and electric field, and n_0 is the averaged density. Thus, in this MHD formulation with the effective resistivity,[48] the Hall effect in the neutral sheet and various fluctuations contribute together to $\eta_{\mathrm{anom}} j_y$.

Looking for the physical cause of the observed anomalous resistivity, the detailed characteristics of the electrostatic and electromagnetic turbulence, dispersion relations, spatial profile, frequency spectrum, etc., have been investigated.[40,41] From the correlation of the potential fluctuation amplitudes with the observed resistivity enhancement, it was concluded that the electrostatic wave does not play a major role in determining the reconnection rate. It has been found that the electromagnetic fluctuations peak at the center of the current sheet. With the use of a hodogram probe,[41] the observed electromagnetic waves have been identified as right-hand polarized whistler waves propagating obliquely to the magnetic field. The dispersion relation of the wave was measured in MRX using the phase shift between two spatial points. A clear correlation has been found between the wave amplitudes and the fast reconnection rate in the low density, collisionless regime.

Recent 2D numerical simulations[32] based on two-fluid or kinetic codes demonstrate the presence of a very thin current layer of width comparable to the electron skin depth, c/ω_{pe}, which is formed inside the reconnection layer (neutral sheet). However, there has not been clear experimental evidence of such a thin current layer ($\delta \sim c/\omega_{pe}$) in laboratory plasmas. For 3D reconnection, there exists a volume of publications of theoretical and numerical studies of fast reconnection including some recent publications.[35,42] At present, there is yet no definite consensus as to the cause of the observed fast reconnection or enhanced resistivity. There are many different levels of approaches in the numerical models (two-fluid, fluid-particle hybrid, full particle simulations, and different 2D or 3D geometries) and many candidate phenomena including the effects of fluctuations (magnetosonic waves, lower-hybrid waves, ion acoustic waves, whistler waves etc.) to explain the observed enhanced resistivity.[29,43] Thus, it is crucial to investigate reconnection in a laboratory setting in which important characteristics can be simultaneously measured *in situ* and compared with numerical simulation results, as well as with analytical theories. Recently, based on MRX data,[41] a series of papers have been published to evaluate the excitation mechanisms and the nonlinear effects of high frequency electromagnetic waves ($\omega > \omega_{ci}$) observed in the neutral sheet.[44,45] These waves can couple with the laminar Hall MHD effects described above to increase the reconnection resistivity and accelerate the reconnection speed. Also it is conceivable that field line breaking at the center of reconnection region can trigger these waves.

III. EXPERIMENTAL SETUP ON THE UPGRADED MRX APPARATUS

The MRX device was built in 1995 to investigate the fundamental physics of magnetic reconnection. Although the overall initial geometry is axisymmetric (and hence two dimensional), it can be made nonaxisymmetric to study 3D characteristics of merging. These plasmas have a high conductivity ($S \sim 10^3$) and are strongly magnetized with the ion gyroradius being much smaller than the plasma size. In 2004, an upgrade of the MRX facility was carried out to increase its capability and to address the physics issues for collisionless reconnection of greatest interest in space, astrophysical and other laboratory applications. Figure 3 shows a recent

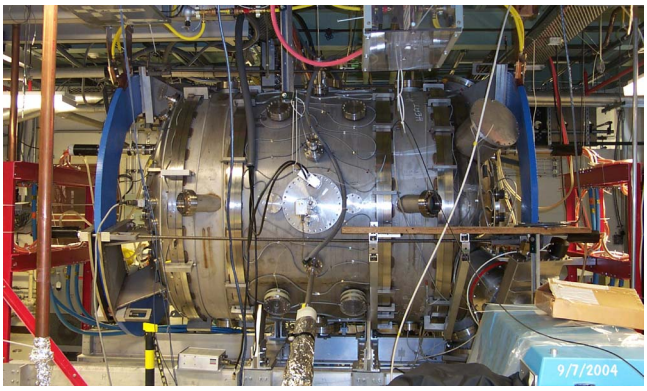

FIG. 3. A photograph of the newly upgraded MRX device.

photograph of MRX taken after the upgrade was completed. The length of the MRX vacuum vessel has been increased to accommodate a variety of separation distances between the two plasma-forming flux cores (from 0.3 to 1.2 m) and allows us to systematically study the effects of the plasma boundary.

The MRX capacitor bank system has been refurbished with the addition of a 0.5 MJ capacitor set. It is expected that the maximum magnetic field strength will be increased together with the time duration of driven reconnection. As the peak electron temperature rises, the Lundquist number is expected to increase up to 10^4 compared with 200-800 in the past experiments. To date, with an increased neutral sheet length, the maximum Lundquist number has already been increased to 2500. The increased temperature will allow the experiment to more freely access the collision-free regime.

The MRX diagnostics consist of internal magnetic and electrostatic probes and noninvasive optical systems as shown in Fig. 4. The relatively short lived, low-temperature MRX plasma has the advantage that Langmuir and magnetic probes can be inserted inside the plasma. Both 1D and 2D arrays of magnetic probes (size $<3-5$ mm) are used in MRX research. By integrating the local magnetic field at a fixed poloidal plane, one can deduce a measured poloidal flux plot during magnetic reconnection. Fine-scale, *in situ*, 1D probe arrays (two 35 channels with resolution up to 2.5 mm and one 71 channels with resolution up to 1.25 mm)

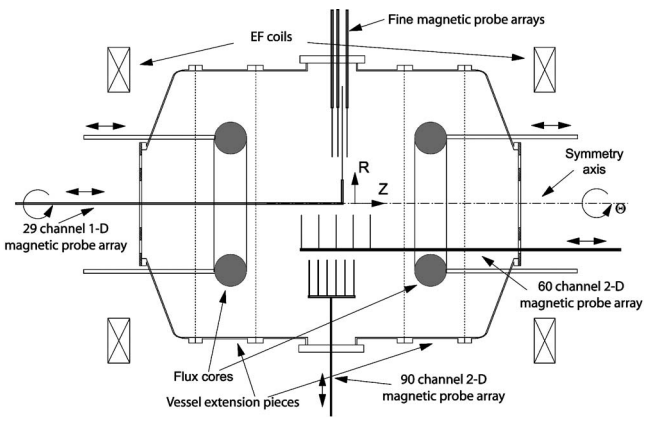

FIG. 4. Experimental setup with the upgraded MRX apparatus

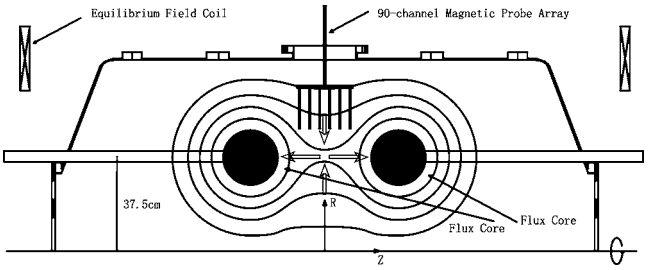

FIG. 5. A schematic view of the pull-driven reconnection without guide field.

have been inserted into the current sheet region to monitor the 2D sheet current profile. The grid size of internal probe arrays varies from 1.25 mm to 4 cm.

The present experimental campaign has been carried out in the double annular plasma configuration in which two toroidal plasmas with annular cross section are formed independently around two flux cores. Magnetic reconnection is driven in the neighborhood of the *X* point of the initial field shown in Fig. 5. Each flux core (darkened section in Figs. 4 and 5) contains a toroidal field (TF) coil and a poloidal field (PF) coil. At first the initial poloidal magnetic field is established by the PF coil currents (which flow in the toroidal direction). Plasma discharges are then created around each flux core by the induction of pulsing currents in the TF coils.[29,30] As plasma is created, the PF coil current is decreased, retracting the poloidal flux to the flux cores. The common flux is thus "pulled" back toward the c.c. point (pull mode) as shown in Fig. 5. For the present research, this "pull" mode of driven reconnection was primarily utilized to study the two-fluid effects of the reconnection dynamics. For normal operating conditions the plasma parameters are: $n_e = 0.1-1\times10^{14}$ cm^{-3}, $T_e = 5-20$ eV, $B = 0.1-0.5$ kG. There is a strongly magnetized global MHD plasma around the reconnection layer. The mean-free path for electron-ion Coulomb collisions can be varied in the range of 0.1–20 cm covering both the collisionless [$\lambda_{mfp} \gg \delta$ (sheet width)] and the collisional ($\lambda_{mfp} \ll \delta$) plasma regimes.

IV. STUDY OF TWO-FLUID PHYSICS IN THE NEUTRAL SHEET OF MRX

In the recent operation of MRX, magnetic reconnection dynamics in the low density regime has been extensively studied to investigate the physics of magnetic reconnection in a regime not dominated by electron-ion collisions. The local features of the reconnection layer are measured by a variety of probe arrays. The 71-channel and 35-channel 1D magnetic probe arrays are inserted radially at various off-center ($Z \neq 0$) positions to measure the radial profile of the out-of-plane magnetic field B_T. The systematic error of the measurements by these probes is less than 10 G. Simultaneously, the coarser 90-channel magnetic probe array is used to measure the three components of magnetic field vector (B_R, B_Z, B_y) at 30 locations in a (R,Z) plane, as illustrated in Fig. 4. We note that the (R,Z,y) coordinate system is employed for the present experimental analysis (y denotes the toroidal direction), instead of the (x,y,z) coordinate system

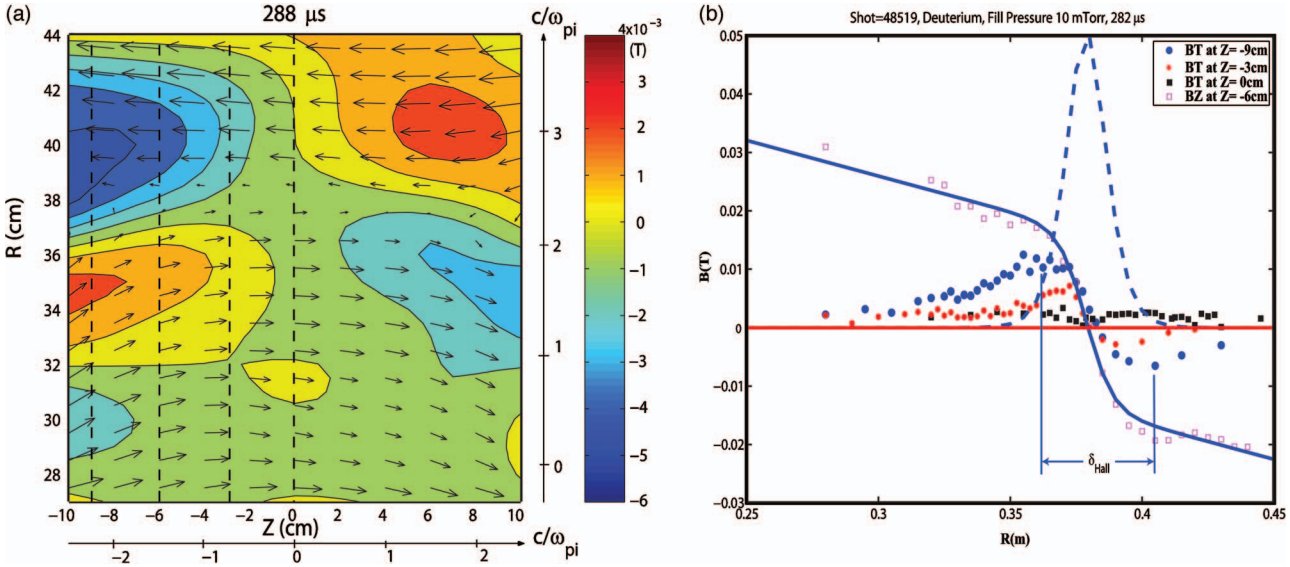

FIG. 6. (Color) (a) The magnetic field in the diffusion region for deuterium plasmas with fill pressure of 5 mTorr. c/ω_{pi} is approximately 4 cm. The arrows depict the measured magnetic field vectors in the $R-Z$ plane. The size of the arrows is normalized to the maximum magnetic field strength, 300 G. The color coded contour plot shows the out-of-plane magnetic field B_T. The dashed lines indicate the coordinates of the linear magnetic probe arrays. (b) The measured out-of-plane magnetic field at $Z=0$ cm (black squares), $Z=-3$ cm (red stars), $Z=-9$ cm (blue dots). The reconnecting magnetic field (magenta squares), fitted Harris profile (solid line) and its toroidal current density profile (dashed line) at $Z=-6$ cm.

used in Fig. 2; $Z \Leftrightarrow z$, $R \Leftrightarrow x$. A separate 29-channel 1D magnetic probe array with spatial resolution of 5 mm is put at $Z=-6$ cm, 6 cm away from the current sheet center plane, to measure the reconnection magnetic field B_Z. By fitting the measured reconnecting field B_z to the Harris sheet profile, the current density profile was calculated.[31] The present series of experiments were performed in Hydrogen, Deuterium and

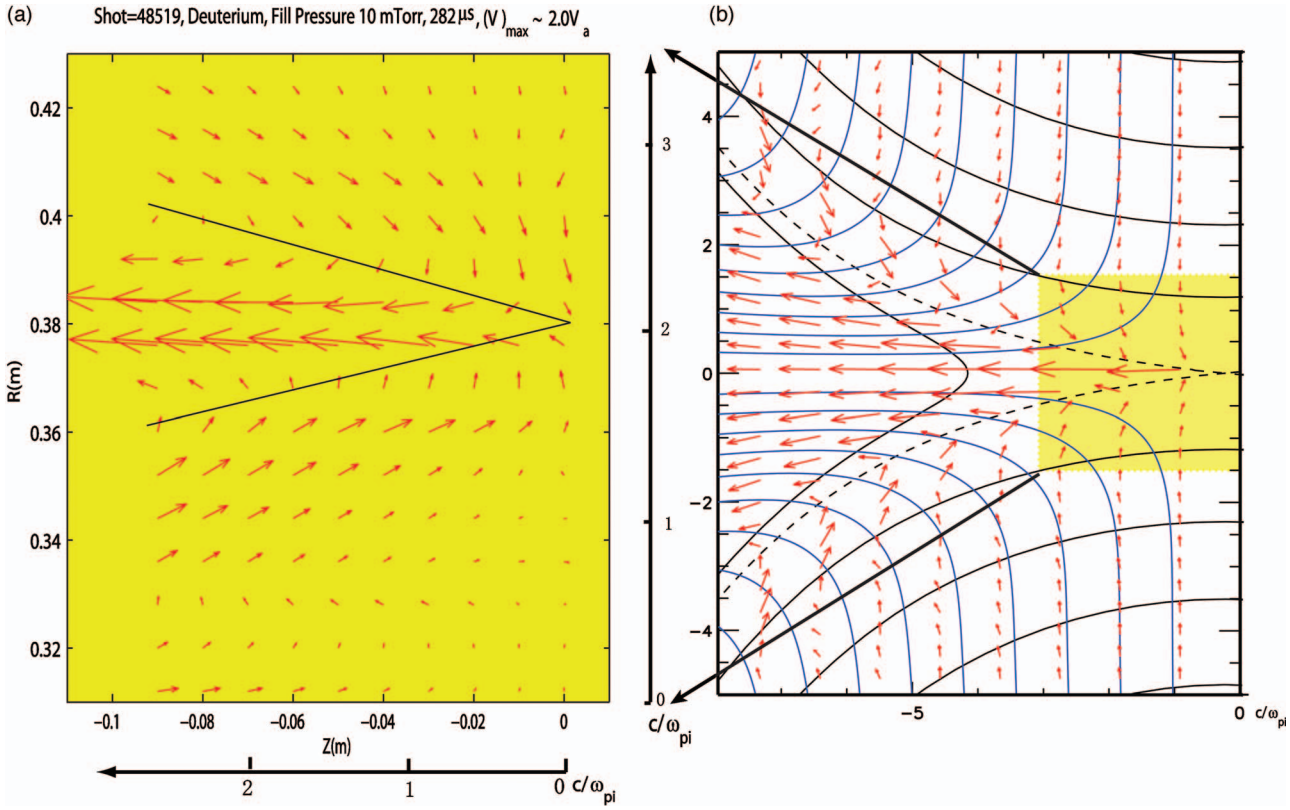

FIG. 7. (Color) Comparison of 2D profiles of Hall (a) current measured in MRX with those from (b) numerical simulation. The green lines show the positions of the separatrixes. (a) should be compared with the yellow-coded region in (b) for the same spatial coverage in terms of c/ω_{pi}. In (b) patterns of ion (blue lines) and electron (red arrows) fluid flows are shown with the flux plot of reconnection field lines (black) just as in Fig. 2(b).

Helium plasmas during "null-helicity" reconnection,[29] where no initial toroidal guide field is applied.

A. Measurement of 2D profiles of the neutral sheet with the Hall effects

The pull mode driven reconnection mode of operation is utilized to investigate the two-fluid effects by inductively driving magnetic flux into the reconnecting neutral sheet in MRX. In this experiment, the pull magnetic reconnection lasts for about 40 μs, much longer than the typical Alfvén time $\tau_A(=L/V_A<1\ \mu s)$ in the MRX plasmas. After the magnetic reconnection process is initiated, an out-of-plane quadrupole magnetic field was observed. It should be noted that the long reconnection duration, achieved due to the upgrade, is a key to the clear observation of the out-of-plane quadruple magnetic field, which only appears after the residual toroidal fields from the initial plasma formation process recede.

We measure the 2D profile of the out-of-plane quadrupole magnetic field by scanning the 90-channel probe array. Figure 6(a) shows the contours of this out of plane quadrupole field in the diffusion region during reconnection, together with the vectors of the reconnection magnetic field in the R,Z plane. The spatial resolution of Fig. 6(a) is 4 cm in the Z direction (grid size) and is improved to 1 cm in the R direction by radially scanning the probe array and averaging several discharges at each position. The quadrupole configuration of the out-of-plane magnetic field B_T is in remarkable agreement with the profile in Fig. 2(b) obtained from a recent numerical calculation.[38]

The measured amplitude of this quadrupole field is typically of the order of 30–50 % of the reconnection field, and sometimes exceeds 60 %. Two characteristic scales for the out-of-plane toroidal field can be defined in Fig. 6(a). L_{Hall} and δ_{Hall} are defined as the distance between two peaks of the quadrupole field in the Z-direction and in the R direction, respectively, and characterize the spatial scales of the quadrupole field in the Z direction and in the R direction. In Fig. 6(b), L_{Hall} is approximately 18–20 cm and δ_{Hall} is approximately 5–6 cm. Taking a typical plasma density of 6×10^{13} cm^{-3} for these discharges, we can calculate the ion skin depth for the deuterium plasma to be approximately 4 cm, yielding $L_{\mathrm{Hall}}\sim5c/\omega_{pi}$ and $\delta_{\mathrm{Hall}}\sim1-1.5c/\omega_{pi}$. This is consistent with numerical simulation results ($\mathrm{L_{Hall}}\sim5c/\omega_{pi}$ and $\delta_{\mathrm{Hall}}\sim c/\omega_{pi}$).[46]

The radial profile of the quadrupole field is measured by the 35-channel and 71-channel probe arrays with higher spatial resolution. Figure 6(b) shows a snapshot of the radial profiles of the out-of-plane toroidal field B_T at $Z=0$, -3, and -9 cm and the reconnection field B_Z and toroidal current density profile j_T at $Z=-6$ cm. The snapshot is taken at a time well after reconnection begins. In Fig. 6(b) the toroidal magnetic fields at $Z=-9$ cm and $Z=-3$ cm reverse sign around the center ($R=37.5$ cm) of the current sheet. The toroidal magnetic field at $Z=0$ does not reverse sign, revealing the quadrupole configuration of the out-of-plane toroidal magnetic field. The measurement of the toroidal magnetic field at $Z=0$ shows a residual field of about 20 G, which is due to the peripheral current outside of reconnection region and is much smaller than the reconnection magnetic field (160 G at the shoulder). The amplitude of the quadrupole toroidal field (B_T) in Fig. 6(b) is about 80 G (The smaller observed amplitude in Fig. 6(a) is due to the coarse spatial resolution of the 2D magnetic probe array). The ratio between the amplitude of B_T and reconnection magnetic field B_Z (at the shoulder) reaches 0.5, showing that a substantial amount of B_T can be generated during magnetic reconnection. In Fig. 6(b), δ_{Hall} is approximately 4 cm which is on the order of c/ω_{pi} (=3.5 cm for this deuterium discharge). The spatial scaling here is again consistent with numerical simulation.[46]

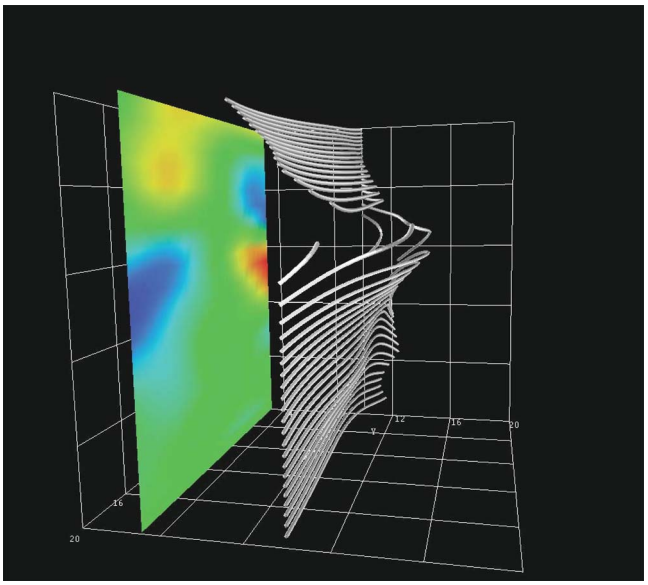

FIG. 8. 3D profiles of reconnecting field lines measured in the MRX neutral sheet. The out-of-plane quadrupole (B_T) is also shown in color coded contours in the projection back screen. It is seen that the 3D magnetic field lines are pulled toward the right by electrons flowing in the y direction, in the neutral sheet.

Figure 7(a) depicts profiles of electron flow (current) in the reconnection plane (x,z), as derived from the out-of-plane quadrupole field assuming ion flows are much smaller than electrons (This assumption is reasonable based on the measured ion flows ($\ll V_A$) in MRX[47]). The out-of-plane magnetic field was again measured by the 71-channel and 35-channel probe arrays. The MRX experimental data show that as electrons flow through the separatrix regions of reconnection sheet, they are first accelerated toward the X point (center of the reconnection plane). After making a sharp turn at the separator lines, they then flow outward in the z direction. Figure 7(b) shows the results from a numerical simulation.[38] When one compares the corresponding flow patterns between the MRX experimental data and the numerical simulation (in yellow section), one finds that the agreement is excellent and that the data illustrates the essence of the Hall effects. The vectors of electron flow in MRX illustrate that, after the initial acceleration, electrons are further accelerated as they pass through the narrow channel section around the central separtrix. The initial acceleration may be due to a larger $E\times B(\sim E_y/B_z)$ velocity as the

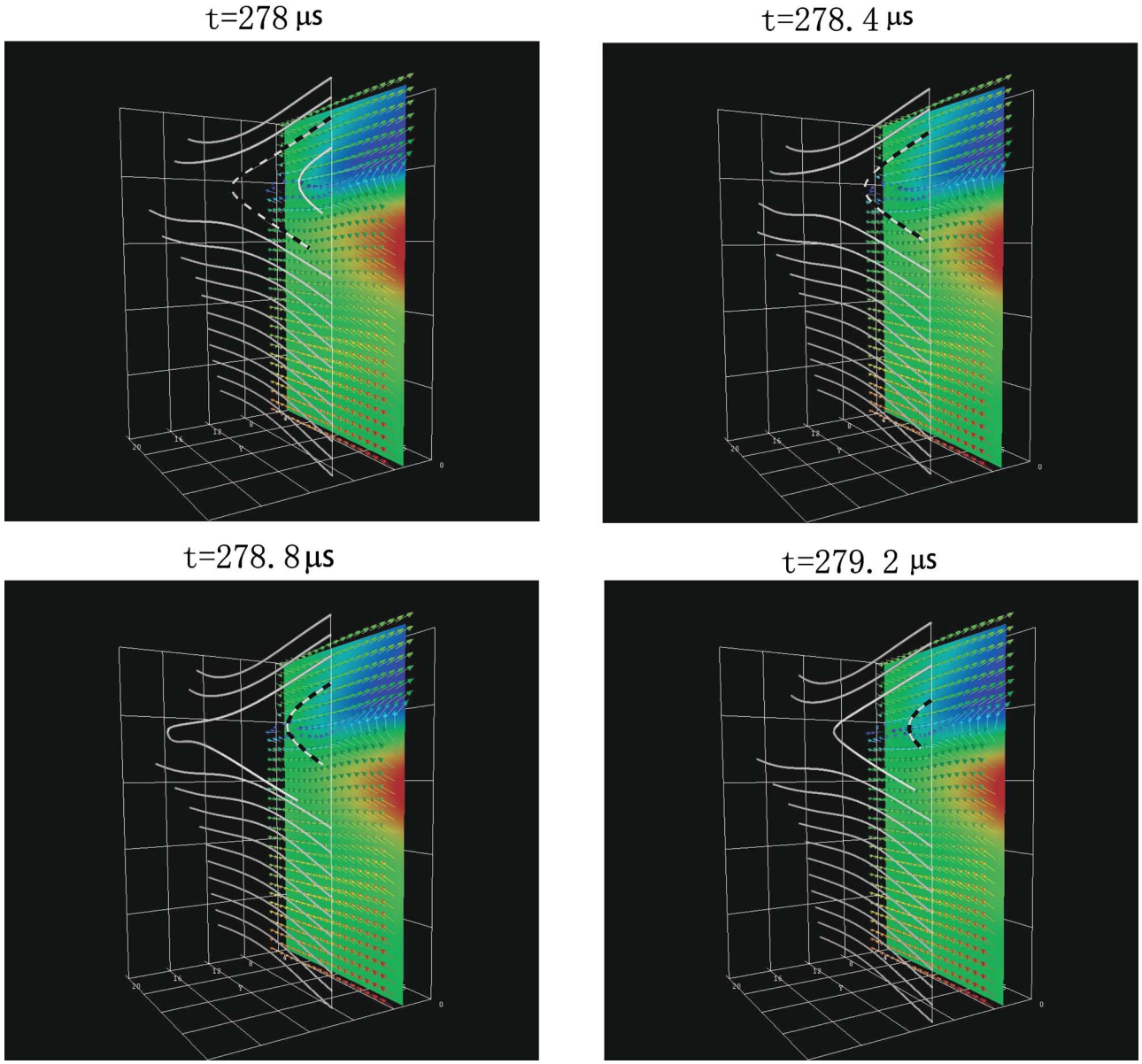

FIG. 9. Evolution of 3D profiles of reconnection field lines measured in one half of the MRX neutral sheet using four fine structure probe arrays shown in Fig. 6(a). The out-of-plane quadrupole (B_y) is also shown in color coded contours in the projection back screen. The electron sheet current pulls the field lines to the left.

reconnection magnetic field diminishes near the origin ($B_z \sim 0$) with uniform reconnection electric field, E_y. The electrons are expected to be accelerated further in the x direction by the E_z field created during the reconnection process.

The magnitude of the Z component of the in-plane Hall current density j_Z can be estimated based on this value. From $j_Z \sim B_T/(\mu_0 \delta_{\mathrm{Hall}}/2)$, the magnitude of j_Z is approximately 0.3 MA/m^2. This in-plane current density is sizable compared to the neutral sheet current density ($\sim$0.5 MA/m^2 in the y direction). Further, the electron outflow velocity near the current sheet midplane ($R \sim 38$ cm) can be estimated based on the assumption that the current mostly comes from the electron flow. Using $v_{Ze}=j_Z/(en)$ and $n \sim 8.5 \times 10^{13}$ cm^{-3}, v_{Ze} is approximately 20 km/s. This is comparable to $V_A \sim 25$ km/s based on the shoulder reconnection field and the central density.

B. Three-dimensional display of measured reconnecting field evolution

From the three measured components of the magnetic field, one can display the reconnecting field lines in 3D as shown in Fig. 8. Figure 8 is generated by tracing field lines through B (magnetic field vectors) measured in a $(R-Z)$ plane grid shown in Fig. 6. One can see clearly that the electrons pull magnetic field lines in the direction of the electron sheet current, the yy direction. In making Fig. 8, the toroidal field components of the 90-channel probe were recalibrated by the values more accurately measured by the fine structure probes.

Figure 9 presents a series of movie pictures which describe 3D field line evolution in one half of the reconnection region during reconnection. The data was taken in the

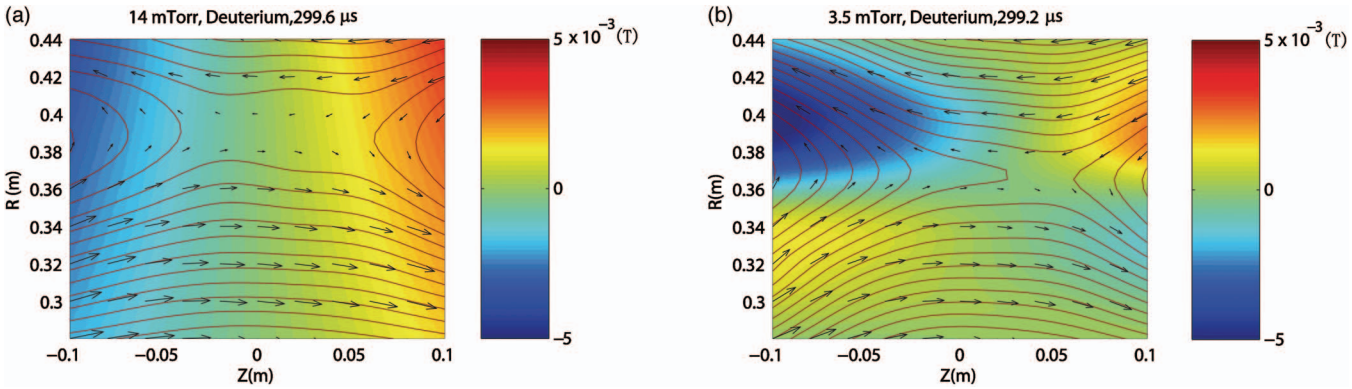

FIG. 10. (Color) Comparison of neutral sheet configuration described by measured magnetic field vectors and flux counters for high (collisional) and low density cases. (a) Collisional regime ($\lambda_{mfp} \sim 1$ mm $\ll \delta$). (b) Near collision-free regime ($\lambda_{mfp} \sim 1$ cm $\sim \delta$). Out-of plane fields are depicted by the color codes ranged -50 G $< Bt < 50$ G.

collision-free regime ($\lambda_{mfp} > \delta$). This movie series was generated from experimental magnetic field data measured by the four fine structure probes (with 0.5 cm resolution in R direction) placed in a (R,Z) plane, as shown by the vertical dots in Fig. 6(a), 0, −3, −6, and −9 cm. In Fig. 9, a designated field line (depicted by broken line) is seen to move out of the center of the reconnecting region in the Z direction after reconnection. It is also seen that the field lines are bent toward the direction of electron flow, namely from right to left in this case. It is found that the reconnection speed increases as the quadrupole field strength increases, as the plasma density is reduced to reach the collisionless regime.

Based on our measurement we can estimate the rate of magnetic field dissipation in the reconnection region by using $W = \mathbf{j} \cdot \mathbf{E} \sim j_y E_y$. We expect the dissipation can be exacerbated by high frequency magnetic fluctuation in the current sheet, as was reported before[44] with $\mathbf{W} \sim j_y E_y$. Based on the measured values of $j_y = 5 \times 10^5$ A/m^2, $E_y = 100$ V/m, $j_y E_y \sim 50$ W/cm^{-3}, using $W = n_e T_e / \tau_{conf}$ and heat loss time of $\tau_{conf} \sim 1$ μs, we could estimate the electron temperature increase of $\delta T_e \sim 6$ eV. In the MRX reconnection, $\delta T_e \sim 3-4$ eV was measured in rough agreement with the previous estimate. This value is much larger than the value $\delta T_e \sim 0.5$ eV based on the Spitzer resistivity of 6×10^{-5} Ω m. The ion heating in these experiments was smaller than previously reported,[47] and is a subject of ongoing investigation.

V. TRANSITION FROM TWO-FLUID TO MHD REGIME

It is observed in MRX that as collisions between ions and electrons increase in frequency, the magnitude of the out-of-plane quadrupole field decreases. This indicates that we are observing a transition from the two-fluid regime to the one-fluid resistive MHD regime. Figure 10 shows how the profile of the MRX neutral sheet changes with respect to collisionality by comparing the neutral sheet configuration described by the measured magnetic field vectors and flux contours for high (collisional) and low density (near collsionfree) cases. In the high plasma density case, shown in Fig. 10(a), where the mean free path is much shorter than the sheet thickness, the out-of-plane field is negligibly small, a rectangular shape flux contour profile of the Sweet-Parker model[1,12,13] is seen, and the classical reconnection rate is measured. There is no recognizable quadrupole field in this case. The weak dipole toroidal field profile seen in Fig. 10(a) depicted by the color contours, is a remnant of the fields created by the initial poloidal discharges around the two flux cores. In the case of low plasma density, shown in Fig. 10(b), where the electron mean free path is longer than the sheet thickness, the Hall MHD effects become dominant as indicated by the out-of-plane field depicted by the color code. A double-wedge shape sheet profile of Petschek type, shown in Fig. 1(b), appears deviating significantly from that of the Sweet-Parker model [Fig. 1(a)], and a fast reconnection rate is measured in this low collisionality regime. However, a slow shock, a signature of Petschek model, has not been identified even in this regime to date.

It is widely known that almost all observed reconnection in laboratory and astrophysical plasmas show much faster reconnection rates than the Sweet-Parker rate. It is important to investigate when two-fluid effects come into play in determining (or accelerating) the reconnection rate. This is believed to happen when the scale size of reconnection regions or local magnetic fluctuations becomes comparable to the ion skin depth. An important parameter is thus the ratio of the ion skin depth to the Sweet-Parker layer thickness, δ_{SP}. In MRX the classical rate of reconnection with the Spitzer resistivity is obtained[43] when the resistivity is large enough to satisfy $c/\omega_{pi} < \delta_{SP}$. When the ion skin depth becomes larger than δ_{SP}, the reconnection layer thickness is expressed by 0.4 c/ω_{pi} (Ref. 31) and the reconnection rate is larger than the classical reconnection rate determined by Spitzer resistivity.

Figure 11 plots relative magnitudes of the Hall electric field normalized by the total reconnection electric field, $[(j_{er} \times B_z)/n_e e]/E_t$ versus δ/λ_{mfp}, the current sheet thickness normalized by the mean free path length of electron-ion collisions. This latter quantity represents a collisionality parameter. As expected from Eq. (1), the contribution of the Hall electric field decreases rapidly as the collisionality increases. As the collisionality increases electrons and ions are expected to move together as a single MHD fluid, and the

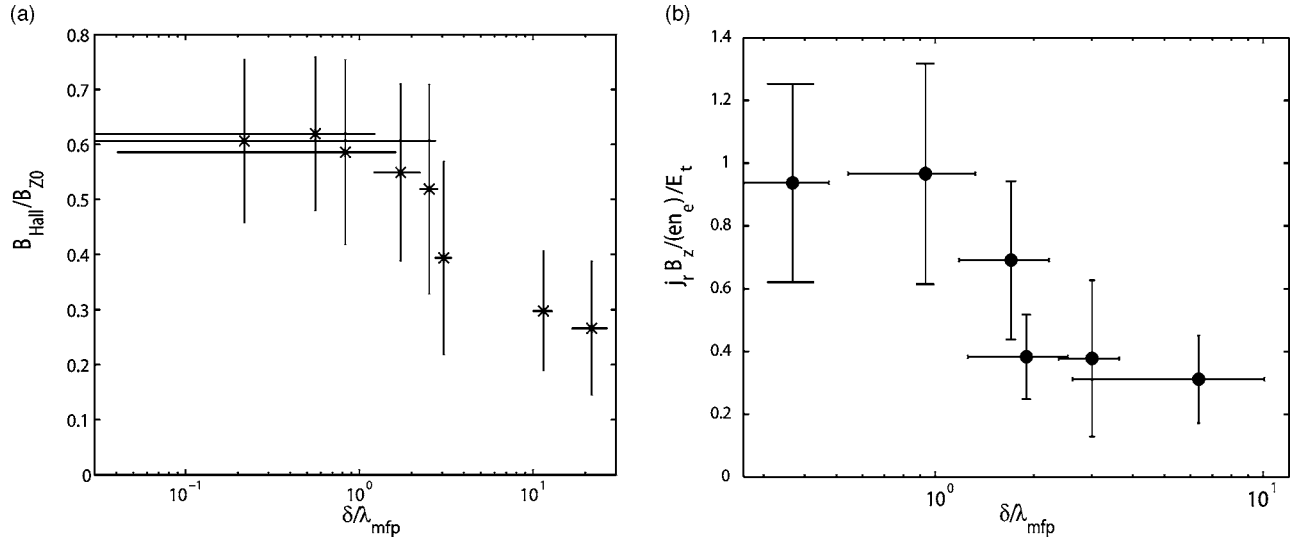

FIG. 11. Relative strength of (a) the Hall field and (b) the contribution of the Hall term ($j_r \times B_z/(en_e)$) to the reconnection electric field are plotted as a function of the collisionality parameter δ/λ_{mfp}. Data are taken in D_2 discharges.

reconnection dynamics can be described by conventional one-fluid MHD.

It is also observed in an intermediate regime of collisionality, $c/\omega_{pe} < \lambda_{mfp} < c/\omega_{pi}$ that the two-fluid MHD effects lead us to a Harris sheet profile[31] in which the thickness can be expressed by

$$\delta_H = \frac{c}{\omega_{pi}} \frac{C_S}{v_d}, \tag{5}$$

where $C_s = [2(T_e + T_i)/M]^{1/2}$ and v_d is the relative drift velocity of the electron sheet current. When the relative drift velocity becomes larger than a certain value, it can induce turbulence in the sheet leading to an enhanced reconnection rate, and we can expect fast reconnection. If we insert the measured values of $v_d/C_s \sim 2.5$, the Harris sheet thickness becomes comparable to the Sweet-Parker width, for $n_e \sim 0.5-1.0 \times 10^{14}$ cm^{-3}. This may suggest that plasma turbulence can be induced for $v_d/C_s > 2.5$ and increase the reconnection rate or that the collision frequency is reduced to a certain threshold value to invoke the Hall effects. It will be determined in the future which mechanism is playing more dominant role. In the high density regime of MRX experiments where a Sweet-Parker reconnection rate is measured, the thickness of the sheet is measured to be $\sim \delta_{SP}$, with $\delta_{SP} > \delta_H$. In the regime of low plasma density, where $\delta_H > \delta_{SP}$, the sheet thickness is found to be always larger than δ_{SP}, and the reconnection rate deviates significantly from that of Sweet-Parker model.[48] It can be concluded that for $c/\omega_{pi} \sim \delta_H > \delta_{SP}$, the neutral sheet cannot be reduced to be the Sweet-Parker width because the two-fluid physics effects would keep the sheet thickness at $\sim 0.4 c/\omega_{pi}$.

A. Criteria for transition from the two-fluid to MHD regime

Let us derive a criterion for the transition from the two-fluid regime where the sheet thickness is generally determined by the ion skin depth,[31] $\delta_i = c/\omega_{pi}$, to the one-fluid collisional MHD regime in which the sheet thickness is determined by Sweet-Parker width, $L/S^{1/2}$. Taking the ratio of the ion skin depth to the Sweet-Parker width, we find

$$\begin{aligned}\delta_i^* = \frac{c}{\omega_{pi}} \frac{1}{\delta_{SP}} &= \frac{\frac{c}{\omega_{pi}}}{L \frac{c}{\omega_{pe}} \sqrt{\left(\frac{2v_{the}}{\lambda_{mfp}} \frac{1}{V_A L}\right)}} \\ &= \left(\frac{m_i}{m_e}\right)^{1/2} \left(\frac{\lambda_{mfp}}{L}\right)^{1/2} \left(\frac{V_A}{2v_{the}}\right)^{1/2} \\ &= \left(\frac{m_i}{4m_e}\right)^{1/4} \left(\frac{\lambda_{mfp}}{L}\right)^{1/2} \left(\frac{V_A}{v_{thi}}\right)^{1/2},\end{aligned} \tag{6}$$

where we have assume $T_e \sim T_i$ and $\eta_\perp = 2\eta_\parallel$. By using $V_A \sim v_{thi} (\beta \sim 1)$ and $m_{iH}/m_e \sim 1800$, this is simplified to

$$\delta_i^* = 4.5 \left(\frac{\lambda_{mfp}}{L}\right)^{1/2} \left(\frac{m_i}{m_{iH}}\right)^{1/4}. \tag{6a}$$

Based on this relationship, it can be argued that when the collision mean free path is long enough to satisfy a condition $\lambda_{mfp} > L/20$ in hydrogen plasma, two fluid effects come into play, making the ion skin depth larger than the Sweet-Parker width to satisfy $\delta_i^* > 1$.

If we calculate this transition condition based on the MRX experimental parameters with system scale $L = 20$ cm, we obtain $\lambda_{mfp} \sim 0.5-1$ cm in MRX. This is consistent with the experimentally measured value within a factor of 2.

B. Observation of the MRX scaling

Figure 12 presents the MRX data for effective *resistivity* $\eta^* = \eta/\eta_{SP}$, $\eta = E/j$ normalized by the Spitzer value η_{SP} in the center of reconnection region[19] in comparison with a scaling obtained in a recent Hall MHD numerical simulation results using a two-fluid MHD code.[38] The horizontal axis represents the ratio of the ion skin depth normalized by the classical Sweet-Parker width ($\delta_{SP} = L/\sqrt{S}$), where L was set

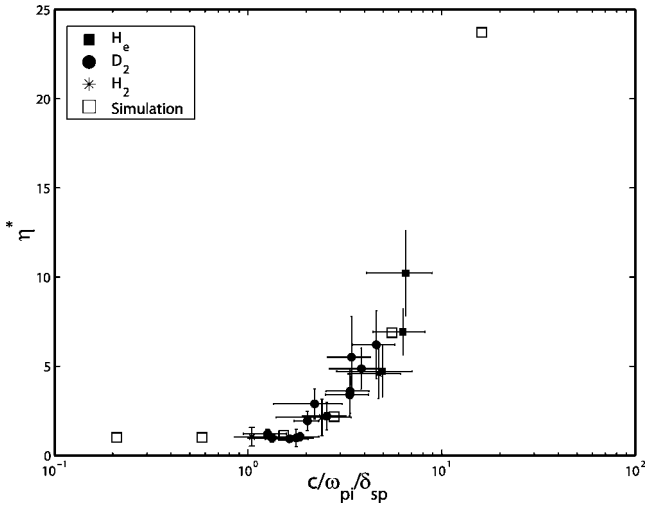

FIG. 12. Effective resistivity $\eta^*=(E/j)$ normalized by the Spitzer value η_{SP} vs the ratio of the ion skin depth to the Sweet Parker width. Effective resistivity measured in MRX are compared with numerical calculation of the contribution of Hall MHD effects to the reconnection electric field. The simulations were based on a 2D two-fluid code (Ref. 38).

to be 20 cm, the system scale. Figure 12 shows that the reconnection resistivity (or reconnection speed) takes off from the classical Spitzer value (or the Sweet-Parker reconnection rate) when the ion skin depth (δ_i) becomes larger than the Sweet-Parker width (δ_{SP}). This MRX scaling indicates that anomalous resistivity is expressed in terms of the laminar Hall effect, when the Spitzer resistivity is not large enough to balance the large reconnecting electric field in fast magnetic reconnection. In the numerical simulation, it was seen that the reconnection electric field primarily comes from the Hall effect, namely $j_{Hall}\times B$ term, and this is consistent with the MRX data shown in Fig. 11. The magnitudes of this laminar Hall effect shown in Fig. 11 peak somewhere outside of the X line. Additional effects, such as anomalous resistivity caused by turbulence, are needed to support reconnecting electric field around the X line and separatrix.[41]We view that both mechanisms, the one based on laminar Hall effect and the other based on turbulence, may be needed.

VI. CONCLUSIONS AND DISCUSSIONS

In the magnetic reconnection experiment (MRX) at PPPL, an extensive study of the two-fluid effects on magnetic reconnection has been carried out in the regime where the electron-ion collision rate is much reduced. An out-of-plane quadrupole magnetic field component has been clearly measured, confirming the presence of two-fluid effects. It is experimentally demonstrated in MRX that magnetized electrons flow differently from ions in the reconnection region and pull magnetic field lines in the direction of electron current. As a result, an out-of-reconnection plane field with a quadrupole profile, a signature of Hall effects, is created as demonstrated in Figs. 6–10. The data set from MRX is in good agreement with the recent two-dimensional simulations, and we believe it is the most conclusive demonstration of the Hall effect in a reconnecting neutral sheet to date.

Recently Uzdensky and Kulsrud[49] developed an analytical theory to describe the characteristics of the out-of-plane quadrupole field generated by the flow of electrons in the reconnection plane. In their model, the ion gyroradius is comparable to the thickness of the layer so that unmagnetized ions present a smooth density throughout a layer while electrons are strongly controlled by the magnetic field. The flow of electrons produces an in-plane current which generates out-of-plane magnetic field. They showed that the resultant field qualitatively agrees with the quadrupole field reported in this paper and that the out-of-plane field is directly proportional to the volume per flux calculated from the midplane. Their calculation shows that the out-of-plane field should increase rapidly as one approached the separatrix where the volume per flux diverges. This rapidly drags the electrons in the neutral sheet current direction due to their flux freezing on to the magnetic field lines. This in turn gives rise to a rather large inertial force in the toroidal direction which can balance the reconnection electric field (E_y) and lead to faster reconnection.

It is important to note that the Hall effect, which occurs due to 2D laminar flows of electrons in the reconnection plane, is observed together with the presence of low and high frequency magnetic turbulence which has 3D structures. This observation in MRX has a striking similarity to magnetospheric measurements of reconnection region, in which the quadrupole component has also been detected together with magnetic fluctuations.[25] This is an important step for identifying the key physics mechanisms for the anomalously fast reconnection which is almost always observed in both laboratory and in space astrophysical plasmas.

It is observed in MRX that the 2D profile of the neutral sheet is changed significantly from the rectangular shape of the familiar Sweet-Parker type[1,12,13] to the double wedge shape similar to that Petschek model,[14] as the collisionality is reduced and reconnection rate increases. Nevertheless, a slow shock has not been identified in MRX. It is observed that when the ion skin depth is larger than δ_{SP}, the reconnection layer thickness is expressed by $0.3-0.5\ c/\omega_{pi}$ in a transition regime from collisional to collisionless[19] and the reconnection rate is larger than the classical reconnection rate based on Spitzer resistivity. In this regime we observe a strong out-of-plane magnetic field together with a large reconnection electric field leading to fast reconnection. When the electron density is increased and the collision-induced resistivity is large enough to satisfy $c/\omega_{pi}<\delta_{SP}$, the rate of reconnection is determined by the Spitzer resistivity, the classical reconnection rate, and the amplitude of the quadrupole field diminishes.

It may be possible to relate the present laboratory results to magnetic reconnection phenomena seen in space and astrophysical plasmas. Table I illustrates the relative ratios of the ion skin depth to the Sweet Parker width for various laboratory and space astrophysical plasmas. If we could extrapolate the present experimental results, we would expect fast reconnection to occur when the relationship of $\delta_i \gg \delta_{SP}$. This inequality holds both in the laboratory and some space plasmas, but not in the interstellar medium plasmas (ISM).

TABLE I. The relative ratios of the ion skin depth to the Sweet Parker width for various laboratory and space astrophysical plasmas.

System	L (cm)	B (G)	$\delta_i = c/\omega_{pi}$ (cm)	δ_{SP} (cm)	δ_i/δ_{SP}
MRX	10	100–500	1–5	0.1–5	0.2–100
RFP/tokamaks	30/100	$10^3/10^4$	10	0.1	100
Magnetosphere	10^9	10^{-3}	10^7	10^4	1000
Solar flare	10^9	100	10^4	10^2	100
ISM	10^{18}	10^{-6}	10^7	10^9	0.01

Most regions of the interstellar medium do not satisfy this condition.

In astrophysical plasmas, there are reconnection regions where two-fluid effects are very important in protostars, in white dwarfs, and in neutron stars.[50] In protostellar disks dust particles of heavy mass are charged positively and ion inertia is increased by collisions with neutrals. The ion skin depth can thus become much larger than the classic Sweet-Parker width, $c/\omega_{pi} > \delta_{SP}$, leading to non-MHD condition where electrons and ions respond differently to the external fields. This implies that Hall terms and electron MHD effects will be important in these environments.

It should be noted that even within the limited two-dimensional reconnection case, the Hall effect alone is not enough to explain the fast reconnection phenomena because of the following two reasons. First, the Hall effect is nondissipative, or in other words it alone cannot dissipate magnetic energy to plasma energy during reconnection. The main function of this effect is to bridge the ion scale dynamics to electron scale dynamics, which can become dissipative through fluctuations. We note that a thin steady electron scale current layers with width comparable to the electron skin depth, which has been identified in two dimensional numerical simulations,[51] has not been observed thus far in MRX. In a realistic 3D geometry, we expect that the electron current layer can break up into broader turbulent structures. Second, the Hall term can become large enough to support the reconnecting electric field, only at locations away from the X line and separatrix, where the laminar component of this term must be small. The magnitudes of this laminar Hall effect shown in Fig. 11 peak somewhere outside of the X line. Additional effects, such as anomalous resistivity, are needed to support the reconnecting electric field around the X line and separatrix. We view that both mechanisms, the one based on laminar Hall effect and the other based on turbulence, may be needed. They are not mutually exclusive, and in fact can be present simultaneously. We also note that the reconnection characteristics are often determined both by the local reconnection physics presented in this paper and the external boundary conditions such as the flux core distances.[52]

Indeed, it was also found previously in MRX that electromagnetic turbulence up to the lower hybrid frequency correlates with the enhanced resistivity,[41] while electrostatic LHDW turbulence does not.[40] Linear and quasilinear theories have been developed to understand the observed turbulence and to evaluate its effects on the dissipation processes.[44,45] During the experiments reported in this paper, the electromagnetic turbulence has also been detected and its correlation with the reconnection rate still holds. We note that the turbulence measurements in MRX have been limited to a few spatial points within the current sheet whereas the out-of-plane quadrupole magnetic field has been observed on a larger scale. The quantitative relationship between the observed out-of-plane quadrupole field and electromagnetic fluctuations is a primary focus of the current MRX research activity, and continues to be studied using a comprehensive set of diagnostics. In particular we plan to investigate the detailed characteristics of obliquely propagating whistler waves as well as lower frequency waves.

ACKNOWLEDGMENTS

Work supported by DOE, NASA and NSF.

[1] E. N. Parker, *Cosmical Magnetic Fields* (Clarendon, Oxford, 1979).
[2] D. Biskamp, *Magnetic Reconnection in Plasmas* (Cambridge University Press, Cambridge, UK, 2000).
[3] J. B. Taylor, Plasma Phys. Controlled Fusion **27**, 1439 (1985).
[4] R. M. Kulsrud, Phys. Plasmas **2**, 1735 (1995); **5**, 1599 (1998).
[5] J. L. Kohl, G. Noci, E. Antonucci *et al.*, Sol. Phys. **175**, 613 (1997).
[6] S. Tsuneta, Astrophys. J. **456**, 840 (1996); **456**, L63 (1996).
[7] S. Masuda, T. Kosugi, H. Hara *et al.*, Nature (London) **371**, 495 (1994).
[8] L. Golub, J. Bookbinder, E. DeLuca *et al.*, Phys. Plasmas **6**, 2205 (1999).
[9] R. P. Lin, S. Krucker, G. J. Hurford *et al.*, Astrophys. J. **595**, L69 (2003).
[10] G. Kivelson and C. T. Russell, *Introduction to Space Physics* (Cambridge University Press, Cambridge, UK, 1995); C. T. Russell and R. C. Elphic, Geophys. Res. Lett. **6**, 33 (1979).
[11] V. M. Vasyliunas, Rev. Geophys. **13**, 303 (1975).
[12] P. A. Sweet, *Electromagnetic Phenomena in Cosmical Physics* (Cambridge University Press, New York, 1958).
[13] E. N. Parker, J. Geophys. Res. **62**, 509 (1957).
[14] H. E. Petschek, NASA Special Publication No. SP-50, NASA, 1964.
[15] T. Hayashi and T. Sato, J. Geophys. Res., [Space Phys.] **83**, 217 (1978); D. A. Uzdensky, Ph.D. thesis, Princeton University, 2000; M. Ugai and T. Tsuda, J. Plasma Phys. **17**, 337 (1977); M. Scholer, J. Geophys. Res., [Space Phys.] **94**, 8805 (1989); D. Biskamp and E. Schwarz, Phys. Plasmas **8**, 4729 (2001).
[16] J. Birn, J. F. Drake, M. A. Shay *et al.*, J. Geophys. Res., [Space Phys.] **106**, 3715 (2001).
[17] B. U. O. Sonnerup, *Solar System Plasma Physics* (North-Holland, New York, 1979).
[18] T. Terasawa, Geophys. Res. Lett. **10**, 475 (1983).
[19] M. Yamada, Earth, Planets Space **53**, 509 (2001).
[20] J. F. Drake and G. R. Burkhart, Geophys. Res. Lett. **19**, 1077 (1992).
[21] M. E. Mandt, R. E. Denton, and J. F. Drake, Geophys. Res. Lett. **21**, 73 (1994).
[22] D. Biskamp, E. Schwarz, and J. F. Drake, Phys. Rev. Lett. **75**, 3850 (1995).
[23] X. H. Deng and H. Matsumoto, Nature (London) **410**, 557 (2001).
[24] M. Oieroset, T. D. Phan, M. Fujimoto *et al.*, Nature (London) **412**, 414 (2001).
[25] F. S. Mozer, S. D. Bale, and T. D. Phan, Phys. Rev. Lett. **89**, 015002 (2002).
[26] Y. Ren, M. Yamada, S. Gerhardt *et al.*, Phys. Rev. Lett. **95**, 055003 (2005).
[27] W. H. Matthaeus *et al.*, Geophys. Res. Lett. **32**, L23 104 (2005); C. D. Cothran *et al.*, Geophys. Res. Lett. **32**, L03105 (2005).
[28] R. L. Stenzel *et al.*, Phys. Plasmas **10**, 2780 (2003).
[29] M. Yamada, H. T. Ji, S. Hsu *et al.*, Phys. Plasmas **4**, 1936 (1997).
[30] M. Yamada, H. T. Ji, S. Hsu *et al.*, Phys. Rev. Lett. **78**, 3117 (1997).
[31] M. Yamada, H. T. Ji, S. Hsu *et al.*, Phys. Plasmas **7**, 1781 (2000).
[32] M. A. Shay and J. F. Drake, Geophys. Res. Lett. **25**, 3759 (1998).
[33] M. Hesse, K. Schindler, J. Birn *et al.*, Phys. Plasmas **6**, 1781 (1999).
[34] R. Horiuchi and T. Sato, Phys. Plasmas **4**, 277 (1997).
[35] P. L. Pritchett and F. V. Coroniti, J. Geophys. Res., [Space Phys.] **109**, (2004).
[36] P. Ricci, J. U. Brackbill, W. Daughton *et al.*, Phys. Plasmas **11**, 4102

(2004).
[37]J. D. Huba and L. I. Rudakov, Phys. Rev. Lett. **93**, 175003 (2004).
[38]Joshua A. Breslau, Ph.D. thesis, Princeton University, 2001; J. A. Breslau and S. C. Jardin, Phys. Plasmas **10**, 1291 (2003).
[39]T. D. Phan, L. M. Kistler, B. Klecker *et al.*, Nature (London) **404**, 848 (2000).
[40]T. A. Carter, H. Ji, F. Trintchouk *et al.*, Phys. Rev. Lett. **88**, 015001 (2002).
[41]H. T. Ji, S. Terry, M. Yamada *et al.*, Phys. Rev. Lett. **92**, 115001 (2004).
[42]R. Horiuchi and T. Sato, Phys. Plasmas **6**, 4565 (1999).
[43]F. Trintchouk, M. Yamada, H. Ji *et al.*, Phys. Plasmas **10**, 319 (2003).
[44]H. Ji, R. Kulsrud, W. Fox, and M. Yamada, J. Geophys. Res., [Space Phys.] **110**, (2005).
[45]R. Kulsrud, H. Ji, W. Fox, and M. Yamada, Phys. Plasmas **12**, (2005).
[46]P. L. Pritchett, J. Geophys. Res., [Space Phys.] **106**, 3783 (2001).
[47]S. C. Hsu, T. A. Carter, G. Fiksel *et al.*, Phys. Plasmas **8**, 1916 (2001).
[48]H. Ji, M. Yamada, S. Hsu *et al.*, Phys. Rev. Lett. **80**, 3256 (1998).
[49]D. A. Uzdensky and R. M. Kulsrud, "Physical Origin of the Quadrupole Out-of-Plane Magnetic Field in Hall-MHD Reconnection," Phys. Plasmas (to be published).
[50]E. G. Zweibel, Astrophys. J. **340**, 550 (1989); E. G. Zweibel and A. Brandenburg, *ibid.* **485**, 920 (1997).
[51]M. A. Shay, J. F. Drake, R. E. Denton *et al.* J. Geophys. Res., [Space Phys.] **103**, 9165 (1998).
[52]A. Kuritsyn, Ph.D. Thesis, Princeton University (2005).